Effect of cell size on the energetics of vacancies in aluminum studied via orbital-free density functional theory

Balachandran Radhakrishnan and Vikram Gavini

Department of Mechanical Engineering, University of Michigan, Ann Arbor, Michigan, 48109 USA

We investigate the effect of cell size on the energetics of vacancies in Aluminum using orbital-free density functional theory with nonlocal kinetic-energy functionals. Extending the recently developed coarse-graining techniques based on quasicontinuum reduction to include nonlocal kinetic-energy functionals, we consider cell sizes up to a million atoms in this study. We find remarkable cell-size effects that are present in computational domains consisting up to $10^3 - 10^4$ atoms, even in simple defects such as vacancies. These results indicate the presence of important long-ranged interactions that have not been considered in prior electronic-structure studies of defects conducted on a few hundred atoms. These cell-size effects are more striking in the computed divacancy binding energies, where vacancies are found to repel each other in small computational cells but become attractive in larger computational cells representative of realistic vacancy concentrations.

PACS number(s): 61.72.jd, 71.15.Mb, 02.70.Dh

I. INTRODUCTION

Defects in materials play a significant role in influencing a wide range of materials properties. Examples include the role of vacancies in creep, spalling, and aging, dislocations in metal plasticity, dopants in semiconductor properties, and domain walls in ferroelectric properties. These defects, though present in small concentrations—for instance, a few parts per million in the case of vacancies—affect material properties at macroscopic scales. In the past decade, many efforts have focused on an electronic-structure study of defects in materials.[1–7] However, due to the computational complexity of electronic-structure theories, these studies have been restricted to periodic geometries with at most a few hundred atoms in most cases. These conventional Fourier space calculations, which have provided tremendous insights into a wide range of materials properties in the past decade, suffer from some important limitations in the study of defects. For instance, the accessible cell-sizes cannot capture the long-ranged nature of elastic and electronic fields that may have a significant influence on the behavior of defects as will be demonstrated in this work. Further, the restrictive assumption of periodicity is not geometrically compatible with the elastic deformations produced by many defects, and thus only artificial configurations of defects, such as quadrapolar arrangement of dislocations, can be studied. Moreover, the small cell-sizes used in electronic structure studies correspond to unrealistically high concentration of defects that are rarely, if ever, realized in nature.

The recent development of the quasicontinuum reduction in orbital-free density functional theory (QC-OFDFT) (Ref. 8) has enabled the consideration of cell-sizes on the order of millions of atoms, thus making possible an electronic-structure study of defect properties using orbital-free density functional theory without cell-size and periodicity restrictions. This quasicontinuum reduction was based on (i) a local variational real-space formulation of the ground-state energy;[9] (ii) a finite-element discretization of the formulation;[9] (iii) an adaptive coarse graining of the finite-element basis providing higher resolution where necessary

while coarsening elsewhere.[8] The method, as an initial demonstration, was developed using the local Thomas-Fermi-Weizsäcker family of kinetic-energy functionals. Using these local kinetic-energy functionals, a study on monovacancy formation energy and divacancy binding energies in aluminum showed cell-size effects up to computational domains containing a few thousand atoms, which are much larger than the conventional cell-sizes considered in vacancy calculations. However, later investigations[10] suggested that the observed large cell-size effects may be a result of the use of inaccurate local kinetic energy functionals, and that such effects may not be present upon the use of the more accurate nonlocal kinetic-energy functionals.[11,12]

In this work, we implement a local real-space formulation of the nonlocal kinetic-energy functionals[11,12] based on the ideas developed in Ref. 13, which then allows the extension of the QC-OFDFT method to include nonlocal kinetic-energy functionals. We subsequently revisit the problem of cell-size effects on monovacancy formation energy and divacancy binding energies in aluminum using the nonlocal kinetic-energy functionals. Results from this study show remarkable cell-size effects on the energetics of vacancies, confirming the previous observations[8] on the presence of long-ranged interactions governing the energetics of defects that have mostly been ignored thus far in electronic structure studies of defects.

II. METHODOLOGY

The ground-state energy in density functional theory is given by (cf., e.g., Ref. 14 and 15)

$$E(u, \mathbf{R}) = T_s(u) + E_{xc}(u) + J(u, \mathbf{R}), \quad (1)$$

where $u = \sqrt{\rho}$ is the square-root electron-density; $\mathbf{R} = \{\mathbf{R}_1, \ldots, \mathbf{R}_M\}$ is the collection of nuclear positions in the system; T_s is the kinetic energy of noninteracting electrons; E_{xc} is the exchange-correlation energy; and J denotes the electrostatic interaction energy between electrons and nuclei. In OFDFT, T_s is modeled using explicit functional forms of

electron density, and the most widely adopted transferable functionals have the following representation[11–13,16,17]

$$T_s(u) = \frac{3}{10}(3\pi^2)^{2/3}\int u^{10/3}(\mathbf{r})d\mathbf{r} + \frac{1}{2}\int |\nabla u(\mathbf{r})|^2 d\mathbf{r} + T_k(u).$$

(2)

In the above expression, the first term is the Thomas-Fermi contribution, the second term represents the von-Weizsäcker correction, and T_k denotes the nonlocal *kernel energy*. In the above expression and those to follow, Hartree atomic units are used unless noted otherwise. The functional form of T_k is given by

$$T_k(u) = \int\int u^{2\alpha}(\mathbf{r})K_{\alpha,\beta}[|\mathbf{r}-\mathbf{r}'|;u(\mathbf{r}),u(\mathbf{r}')]u^{2\beta}(\mathbf{r}')d\mathbf{r}d\mathbf{r}',$$

(3)

where parameters α, β, and the kernel $K_{\alpha,\beta}$ are chosen such that the kinetic-energy functional satisfies the Lindhard susceptibility function in Fourier space (cf., e.g., Ref. 15). Further, based on the dependence or independence of kernel $K_{\alpha,\beta}$ on u, these kernels are often referred to as density-dependent (DD) or density-independent (DI) kernels.[11,12] It is a common practise to decompose the DD kernels into a series of DI kernels through a Taylor expansion about a reference density,[12,13] and a similar treatment is considered in this work.

The various components of energy in Eq. (1) are local in real space, except the electrostatic interaction energy and the kernel energy that are extended in real space. We now proceed to develop a local variational real-space formulation of OFDFT which is central to the coarse-graining techniques introduced subsequently. To this end, following the work in Ref. 9, the electrostatic interactions are reformulated as the following local variational problem

$$J(u,\mathbf{R}) = -\min_{\phi}\int\left[\frac{1}{8\pi}|\nabla\phi(\mathbf{r})|^2 - (u^2(\mathbf{r})+b(\mathbf{r};\mathbf{R}))\phi(\mathbf{r})\right]d\mathbf{r}$$

(4)

by taking recourse to the Poisson equation and estimating the electrostatic potential ϕ of the charge distribution. In the above expression, $b(\mathbf{r};\mathbf{R})$ denotes a regularized nuclear charge distribution, which, in pseudopotential calculations, represents a nuclear charge distribution corresponding to a pseudopotential. We now consider the local reformulation of the nonlocal kernel energies. We present the formulation in the context of DI kernel energies, and DD kernel energies are reformulated in a similar manner. To this end, we define the following potentials:

$$V_\alpha(\mathbf{r}) = \int K_{\alpha,\beta}(|\mathbf{r}-\mathbf{r}'|)u^{2\alpha}(\mathbf{r}')d\mathbf{r}',$$

$$V_\beta(\mathbf{r}) = \int K_{\alpha,\beta}(|\mathbf{r}-\mathbf{r}'|)u^{2\beta}(\mathbf{r}')d\mathbf{r}'.$$

(5)

Taking the Fourier transform of the above expressions, we obtain, $\hat{V}_\alpha(\mathbf{k}) = \hat{K}_{\alpha,\beta}(\mathbf{k})\widehat{u^{2\alpha}}(\mathbf{k})$, $\hat{V}_\beta(\mathbf{k}) = \hat{K}_{\alpha,\beta}(\mathbf{k})\widehat{u^{2\beta}}(\mathbf{k})$. Fol-

lowing the ideas developed in Ref. 13, $\hat{K}_{\alpha,\beta}$ can be approximated to very good accuracy using a sum of partial fractions of the following form:

$$\hat{K}_{\alpha,\beta}(\mathbf{k}) \approx \sum_{j=1}^{m}\frac{A_j|\mathbf{k}|^2}{|\mathbf{k}|^2+B_j},$$

(6)

where A_j, B_j, $j=1,\ldots,m$ are constants, possibly complex, that are determined using a best fit approximation (cf., Ref. 13). We now define

$$\hat{V}_{\alpha_j}(\mathbf{k}) = \frac{A_j|\mathbf{k}|^2}{|\mathbf{k}|^2+B_j}\widehat{u^{2\alpha}}(\mathbf{k}) \quad j=1,\ldots,m,$$

(7a)

$$\hat{V}_{\beta_j}(\mathbf{k}) = \frac{A_j|\mathbf{k}|^2}{|\mathbf{k}|^2+B_j}\widehat{u^{2\beta}}(\mathbf{k}) \quad j=1,\ldots,m.$$

(7b)

Taking Fourier transform of Eq. (7), we obtain a system of Helmholtz equations given by

$$-\nabla^2 V_{\alpha_j}(\mathbf{r}) + B_j V_{\alpha_j}(\mathbf{r}) + A_j\nabla^2 u^{2\alpha}(\mathbf{r}) = 0 \quad j=1,\ldots,m,$$

(8a)

$$-\nabla^2 V_{\beta_j}(\mathbf{r}) + B_j V_{\beta_j}(\mathbf{r}) + A_j\nabla^2 u^{2\beta}(\mathbf{r}) = 0 \quad j=1,\ldots,m.$$

(8b)

Under the approximation given by Eq. (6), the potentials in Eq. (5) now reduce to $V_\alpha(\mathbf{r}) = \sum_{j=1}^{m}V_{\alpha_j}(\mathbf{r}), V_\beta(\mathbf{r}) = \sum_{j=1}^{m}V_{\beta_j}(\mathbf{r})$. By defining $\omega_{\alpha_j}(\mathbf{r}) = V_{\alpha_j}(\mathbf{r}) - A_j u^{2\alpha}(\mathbf{r})$ and $\omega_{\beta_j}(\mathbf{r}) = V_{\beta_j}(\mathbf{r}) - A_j u^{2\beta}(\mathbf{r})$ for $j=1\ldots m$, which we refer to as *kernel potentials*, we rewrite Eq. (8) in terms of these kernel potential to obtain the following Helmholtz equations

$$-\nabla^2\omega_{\alpha_j}(\mathbf{r}) + B_j\omega_{\alpha_j}(\mathbf{r}) + A_j B_j u^{2\alpha}(\mathbf{r}) = 0 \quad j=1,\ldots,m,$$

(9a)

$$-\nabla^2\omega_{\beta_j}(\mathbf{r}) + B_j\omega_{\beta_j}(\mathbf{r}) + A_j B_j u^{2\beta}(\mathbf{r}) = 0 \quad j=1,\ldots,m.$$

(9b)

Expressing these Helmholtz equations in a variational form, we reformulate the nonlocal kernel energies in Eq. (3) as the following local saddle-point problem:

$$T_k(u) = \min_{\omega_{\alpha_j}}\max_{\omega_{\beta_j}}\sum_{j=1}^{m}\left\{\int\left[\frac{1}{A_j B_j}\nabla\omega_{\alpha_j}(\mathbf{r})\cdot\nabla\omega_{\beta_j}(\mathbf{r})\right.\right.$$

$$+\frac{1}{A_j}\omega_{\alpha_j}(\mathbf{r})\omega_{\beta_j}(\mathbf{r}) + \omega_{\beta_j}(\mathbf{r})u^{2\alpha}(\mathbf{r}) + \omega_{\alpha_j}(\mathbf{r})u^{2\beta}(\mathbf{r})$$

$$\left.\left.+A_j u^{2(\alpha+\beta)}(\mathbf{r})\right]d\mathbf{r}\right\}.$$

(10)

Using the local reformulations of the extended interactions in Eqs. (4) and (10), the ground-state energy in OFDFT can now be expressed as a local variational problem in real-space with the independent variables comprising of the positions of nuclei ($\mathbf{R}$), and the *electronic fields* constituted by square-root electron-density (u), electrostatic potential (ϕ), and the kernel potentials ($\omega_{\alpha_j}, \omega_{\beta_j}, j=1,\ldots,m$). We employ a finite-

TABLE I. Bulk properties of Aluminum.

Properties	KSDFT (Refs. 12 and 13)	OF-FS (DI) (Ref. 11)	OF-RS (DI)	OF-FS (DD) (Ref. 12)	OF-RS (DD)
Bulk modulus (GPa)	68.5	71.9	72	72	71.72
Energy per atom (eV)	−58.33	−58.33	−58.38	−58.33	−58.33
Lattice constant (a.u.)	7.62	7.59	7.58	7.61	7.6

element basis,[18] which is consistent with the local and variational structure of the formulation, to numerically obtain the ground-state solution. To test the viability of the proposed approach, we first computed the bulk properties of aluminum. We conducted the study for both DI kernel energy with $\{\alpha,\beta\} = \frac{5}{6} \pm \frac{\sqrt{5}}{6}$ and the Wang-Govind-Carter Density-Dependent (WGC-DD) kernel energy[12] which is a widely used kinetic energy functional in OFDFT to describe aluminum. In all our studies, the kernels are approximated by a sum of four partial fractions [$m=4$ in Eq. (6)], and the sufficiency of this approximation will be demonstrated from the results (cf. Table I). In the case of WGC-DD model, the kernel energy is expanded about the average bulk electron density. We used the local-density approximation for exchange correlation energies[19] and the Goodwin-Needs-Heine pseudopotential for aluminum (Ref. 20) in all our computations. The computed bulk properties of aluminum using the proposed real-space formulation (OF-RS) are tabulated in Table I, and are in good agreement with other calculations using conventional Fourier-space techniques in OFDFT (OF-FS) as well as Kohn-Sham density functional theory (KS-DFT).

We now present the key ideas behind the coarse-graining techniques that enable electronic-structure calculations on multimillion atoms systems at no significant loss of accuracy, and refer to Ref. 8 for a more comprehensive discussion of these ideas. These coarse-graining techniques based on QC reduction were initially developed in the context of OFDFT with local kinetic-energy functionals,[8] and are extended here to include the nonlocal interactions by coarse graining the additional electronic fields represented by the kernel potentials. In the presence of defects, both displacements of nuclei and electronic fields vary rapidly near the defect core. However, away from the defect core the displacement fields are smooth and vary only on a macroscopic length scale, and in these regions the electronic fields are locally periodic[21]—i.e., electronic fields exhibit the periodicity of the underlying lattice which changes only on a macroscopic length-scale. This structure is exploited to develop the QC reduction in the formulation. First, the displacement fields are resolved using a finite-element triangulation (atomic mesh) of selected nuclei called representative nuclei, and interpolating the positions of all nuclei using the positions of these representative nuclei [Fig. 1(a)]. The representative nuclei are chosen such that all nuclei are resolved near the defect core whereas away from defect core, where the displacement fields are smooth, the resolution becomes coarser and a small fraction of the nuclei is used to determine the positions of the rest. We now turn to the representation and coarse graining of electronic fields that exhibit subatomic oscillations. The electronic fields are decomposed into predictor fields and corrector fields. The predictor fields are represented on a finite-element triangulation of unit cells (auxiliary mesh) residing inside each element of the atomic mesh, and are computed using a periodic calculation with the deformation of the underlying lattice [Fig. 1(b)]. The predictor fields accurately capture the locally periodic electronic structure away from the defect core but provide a very inaccurate representation of the electronic structure close to the defect core. The corrector fields, which correct for these inaccuracies, are thus represented on a finite-element triangulation (electronic mesh) that is sub-atomic close to the defect core and coarse grains away to become superatomic [Fig. 1(c)]. As a matter of convenience, the electronic mesh is chosen to be a uniform subdivision of the atomic mesh, thus increasing the resolution in the corrector fields with increasing resolution in the displacement field. Using this decomposition, the independent variables of the formulation reduce to the coarse-grained variables comprising of the representative nuclei and corrector electronic fields, which are computed using the proposed local real-space variational formulation.

In order to asses the efficiency and the accuracy of the proposed coarse-graining techniques using QC reduction, we computed the monovacancy formation energy in aluminum using a cell-size containing 16 384 nominal number of atoms with differing levels of coarse graining that is controlled by the number of representative nuclei. The results of this study for OFDFT models with DI kernel ($\{\alpha,\beta\} = \frac{5}{6} \pm \frac{\sqrt{5}}{6}$) and
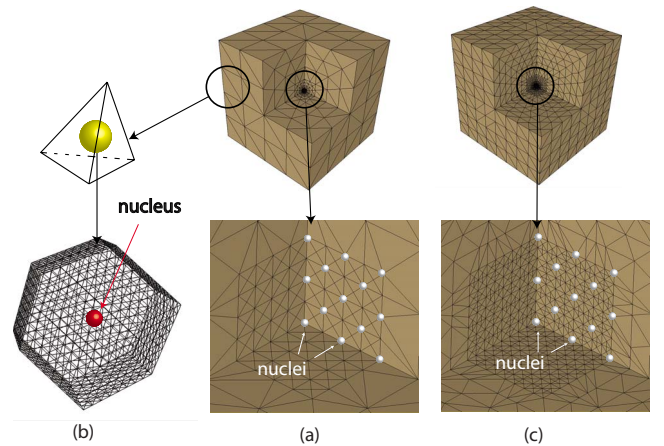

FIG. 1. (Color online) (a) Atomic mesh used to interpolate positions of nuclei away from the fully resolved defect core. (b) Auxiliary mesh used to sample the predictor fields within a unit cell. (c) Electronic mesh used to represent the corrector fields. It has sub-atomic resolution in the defect core, and coarsens away from the defect core.
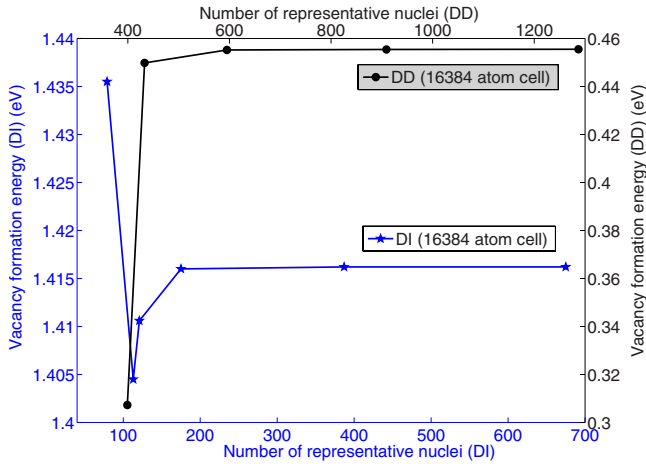
FIG. 2. (Color online) Convergence of coarse-graining approximation.

WGC-DD kernel are shown in Fig. 2. As is evident, less than 200 representative nuclei in the case of DI kernel, and less than 600 representative nuclei in the case of WGC-DD kernel are sufficient to obtain convergence with respect to the coarse graining. This significant reduction in the computational cost afforded by the proposed QC reduction makes possible an electronic structure study of defects without cell-size restrictions, where defects can be studied under naturally occurring concentrations in real materials.

III. CELL-SIZE EFFECTS

We now proceed to investigate the cell-size effects in the energetics of vacancies. To this end, using both DI and WGC-DD OFDFT models, we computed the monovacancy formation energy in aluminum for varying cell-sizes from 32 atoms to a million atoms, and these results are shown in Fig. 3. In the case of WGC-DD model, the kernel energy is expanded about the average bulk electron-density before introducing the vacancy. Homogeneous Dirichlet boundary conditions are imposed on the corrector electronic fields as well as the displacement fields in all computations, which imply
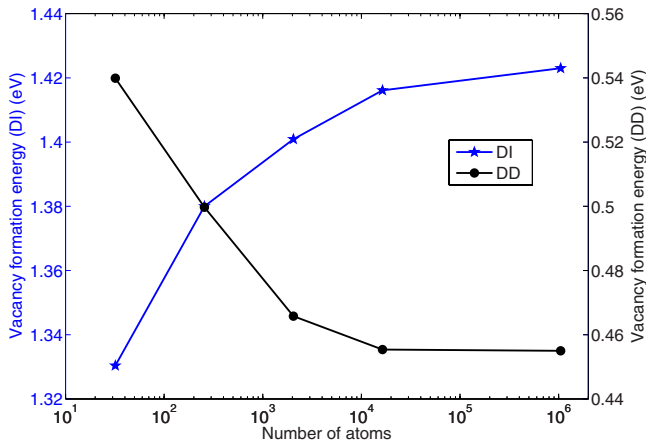

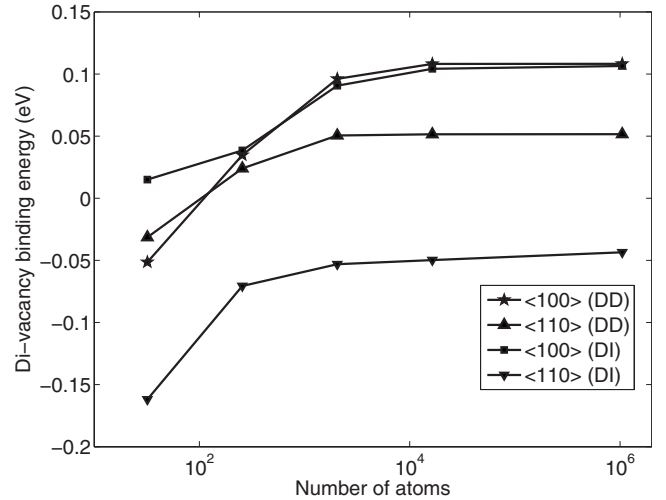FIG. 3. (Color online) Cell-size effects in monovacancy formation energy.

FIG. 4. Cell-size effects in the binding energies of divacancies.

that the perturbations in electronic and displacement fields in the presence of these defects vanish on the boundaries of the sample. The numerical parameters including mesh size and coarse-graining rates are chosen such that the numerical error in computed formation energies is less that 0.01 eV. The monovacancy formation energy computed using a 32 atoms computational cell is 1.33 eV for DI model and 0.54 eV for WGC-DD model, and these results are in very good agreement with those reported in the literature.[10,12] DI kernels are known to be inaccurate in predicting the monovacancy formation energy in aluminum, which is estimated to be 0.51 eV using KSDFT on a 32 atoms computational cell[10] and 0.66 eV from experiments.[22] However, in this study, we focus our attention on the cell-size effects. As seen from Fig. 3, there is a remarkable cell-size dependence in the computed formation energy of a vacancy. These results indicate that cell-sizes on the order of 10^3–10^4 atoms are required to obtain convergence with respect to cell-size even in simple defects such as vacancies. We attribute these cell-size effects to the long-ranged nature of the displacement fields, which is well known from studies on defects using continuum elasticity,[23–25] as well as the slower than expected decay in the perturbations of electronic fields arising in the presence of defects. Linear response theory suggests that the perturbations in electronic fields decay exponentially away from the defect-core, which is often referred to as screening.[26] However, our numerical calculations suggest that nonlinear effects dominate up to a distance of 2–3 lattice units away from the vacancy-core, only beyond which the expected exponential decay is observed. Moreover, the perturbations in the electronic fields are strong enough to be felt up to a distance of 5 lattice units from the vacancy.

The difference in monovacancy formation energies computed using a commonly used 32 atoms cell-size and the more realistic dilute limit corresponding to a million-atoms cell-size is on the order of 0.1 eV, which may appear insignificant at first. However, we note that the interaction energies between vacancies are on the order of 0.1 eV and are significantly influenced by these cell-size effects. Figure 4 shows the cell-size dependence of the ⟨100⟩ and ⟨110⟩ diva-

cancy binding energies in aluminum, which is more striking. In the case of WGC-DD OFDFT model, whose accuracy and transferability has been verified by many numerical studies and comparisons with KSDFT,[10,12] the binding energies are computed to be negative (repulsive) for small cell-sizes while becoming positive (attractive) for larger cell-sizes corresponding to realistic vacancy concentrations of a few parts per million. Thus, the cell-size effects not only change the energetics quantitatively but even change the physics qualitatively.

IV. CONCLUSIONS

In conclusion, this study unambiguously establishes the significant cell-size effects in the energetics of vacancies by using the transferable WGC-DD OFDFT model for aluminum. Results from this study suggest that perturbations in elastic and electronic fields which develop in the presence of defects are long ranged, and, even in the case of simple defects such as vacancies, are felt in cell-sizes containing up to $10^3 - 10^4$ atoms. These long-ranged fields are found to influence the energetics of vacancies both quantitatively as well as qualitatively. It is more likely than not that similar, or stronger, cell-size effects may be present in defects such as dislocations, surfaces and interfaces, and an accurate electronic-structure study of these defects should account for the physical interactions occurring on multiple length scales.

The reliability of WGC-DD OFDFT model in aluminum has been established in the literature by benchmarking the predictions on a wide range of periodic and defect properties with KSDFT calculations.[7,10] Thus, we expect that similar cell-size effects may be present in energetics of vacancies computed using KSDFT. But, an accurate cell-size study with KSDFT to verify this will require the development of coarse-graining techniques for KSDFT, which poses nontrivial challenges due to the delocalized nature of the wave functions and is currently a topic of investigation. Nevertheless, prior to the development of such coarse-graining techniques for KSDFT, QC-OFDFT with WGC-DD kinetic energy functionals can be used to study various aspects of the energetics of defects in aluminum without any cell-size restrictions. These include the computation of formation energies, migration energies, interaction energies of various defects such as dislocations, surfaces, twin boundaries, which can then be used to develop more accurate mesoscopic models of deformation and failure in metals.

[1] S. Ismail-Beigi and T. A. Arias, Phys. Rev. Lett. **84**, 1499 (2000).

[2] H. Üstünel, D. Roundy, and T. A. Arias, Phys. Rev. Lett. **94**, 025503 (2005).

[3] G. Lu and E. Kaxiras, Phys. Rev. Lett. **89**, 105501 (2002).

[4] G. Lu and E. Kaxiras, Phys. Rev. Lett. **94**, 155501 (2005).

[5] Z. Chen, N. Kioussis, N. Ghoniem, and D. Seif, Phys. Rev. B **81**, 094102 (2010).

[6] J. X. Zheng, G. Ceder, T. Maxisch, W. K. Chim, and W. K. Choi, Phys. Rev. B **75**, 104112 (2007).

[7] I. Shin, A. Ramasubramaniam, C. Huang, L. Hung, and E. A. Carter, Philos. Mag. **89**, 3195 (2009).

[8] V. Gavini, K. Bhattacharya, and M. Ortiz, J. Mech. Phys. Solids **55**, 697 (2007).

[9] V. Gavini, J. Knap, K. Bhattacharya, and M. Ortiz, J. Mech. Phys. Solids **55**, 669 (2007).

[10] G. Ho, M. T. Ong, K. J. Caspersen, and E. A. Carter, Phys. Chem. Chem. Phys. **9**, 4951 (2007).

[11] Y. A. Wang, N. Govind, and E. A. Carter, Phys. Rev. B **58**, 13465 (1998).

[12] Y. A. Wang, N. Govind, and E. A. Carter, Phys. Rev. B **60**, 16350 (1999).

[13] N. Choly and E. Kaxiras, Solid State Commun. **121**, 281 (2002).

[14] R. Parr and W. Yang, *Density-Functional Theory of Atoms and Molecules* (Oxford University Press, New York, 1989).

[15] M. Finnis, *Interatomic Forces in Condensed Matter* (Oxford University Press, New York, 2003).

[16] L.-W. Wang and M. P. Teter, Phys. Rev. B **45**, 13196 (1992).

[17] E. Smargiassi and P. A. Madden, Phys. Rev. B **49**, 5220 (1994).

[18] S. C. Brenner and L. R. Scott, *The Mathematical Theory of Finite Element Methods* (Springer-Verlag, New York, 2002).

[19] J. P. Perdew and A. Zunger, Phys. Rev. B **23**, 5048 (1981).

[20] L. Goodwin, R. J. Needs, and V. Heine, J. Phys.: Condens. Matter **2**, 351 (1990).

[21] X. Blanc, C. L. Bris, and P. L. Lions, Arch. Ration. Mech. Anal. **164**, 341 (2002).

[22] W. Triftshäuser, Phys. Rev. B **12**, 4634 (1975).

[23] J. D. Eshelby, in *Solid State Physics, Advances in Research and Applications*, edited by F. Seitz and D. Turnbull (Academic Press, New York, 1956), Vol. III, pp. 79–144.

[24] T. Mura, *Micromechanics of Defects in Solids* (Kluwer Academic, New York, 1987).

[25] R. Phillips, *Crystals, Defects, and Microstructure: Modelling Across Scales* (Cambridge University Press, New York, 2001).

[26] N. W. Ashcroft and N. D. Mermin, *Solid State Physics* (Brooks Cole, Belmont, 1976).